

$\tau_{c||(\text{MX})}$  and  $\tau_{c\perp(\text{MX})}$  values according to Perrin.<sup>36</sup> The results are summarized in Table III.<sup>28</sup>

In the case of  $\text{X}^{n-} = \text{SO}_4^{2-}$ , the values of  $r_{l(\text{MX})}$  and  $r_{s(\text{MX})}$  derived from relaxation experiments were close to the sum of the radii of  $[\text{Co}(\text{en})_3]^{3+}$  and  $\text{SO}_4^{2-}$  and to the  $[\text{Co}(\text{en})_3]^{3+}$  radius, respectively. These results are consistent with the model that the  $[\text{Co}(\text{en})_3]^{3+}\cdot\text{SO}_4^{2-}$  ion pairs are mostly contact ion pairs, which are rotating like a rigid prolate as shown in Figure 5 at least for the order of  $10^{-10}$  s. In each case of  $\text{X}^{n-} = \text{suc}^{2-}$  and  $\text{L-tart}^{2-}$ , the  $r_{l(\text{MX})}$  value from relaxation experiments is somewhat smaller than the sum of the  $[\text{Co}(\text{en})_3]^{3+}$  and  $\text{X}^{n-}$  radii, while the  $r_{s(\text{MX})}$  value is slightly larger than the  $[\text{Co}(\text{en})_3]^{3+}$  radius and slightly smaller than the  $\text{X}^{n-}$  radius. The smaller  $r_{l(\text{MX})}$  value may be interpreted as resulting from the relative lability of the structure of these ion pairs compared with the  $[\text{Co}(\text{en})_3]^{3+}\cdot\text{SO}_4^{2-}$  ion pair; the labile structure may cause a reduction in the effective length of the longer axis of the ellipsoid of the ion pair. The case of  $\text{X}^{n-} = \text{AcO}^-$  may also be explained in a similar manner except that the  $r_{s(\text{MX})}$  value was equal to the  $[\text{Co}(\text{en})_3]^{3+}$  radius because of the smaller radius of the acetate ion.<sup>38</sup> Contrary to the above cases, the ion pair with  $\text{ClO}_4^-$  shows  $r_{l(\text{MX})}$  and  $r_{s(\text{MX})}$  values

approximately equal to the radius of  $[\text{Co}(\text{en})_3]^{3+}$ . This indicates that the lifetime of the ion-pair structure is smaller than  $\tau_{c||(\text{MX})}$  and  $\tau_{c\perp(\text{MX})}$ , or that no directed interaction exists between the ions of the ion pair. At any rate, the  $\text{ClO}_4^-$  ion scarcely gives friction for the rotational diffusion of the  $[\text{Co}(\text{en})_3]^{3+}$  ion in the ion pair. For the ion pairs with  $\text{Cl}^-$  and  $\text{I}^-$ , the situation is more or less similar to the last case, although a slight influence of ion pairing is indicated.<sup>38</sup>

**Acknowledgment.** We thank Dr. Y. Yoshikawa for providing unpublished numerical values for the structure of the  $[\text{Co}(\text{en})_3]^{3+}$  ion. This work was partially supported by Grant-in-Aid for Scientific Research No. 56470039 from the Ministry of Education, Science, and Culture, Japan.

**Registry No.**  $[\text{Co}(\text{en})_3]^{3+}\text{ClO}_4^-$ , 52672-84-1;  $[\text{Co}(\text{en})_3]^{3+}\text{Cl}^-$ , 18372-70-8;  $[\text{Co}(\text{en})_3]^{3+}\text{I}^-$ , 31011-74-2;  $[\text{Co}(\text{en})_3]^{3+}\text{AcO}^-$ , 87461-87-8;  $[\text{Co}(\text{en})_3]^{3+}\text{suc}^{2-}$ , 87461-88-9;  $[\text{Co}(\text{en})_3]^{3+}\text{L-tart}^{2-}$ , 62109-98-2;  $[\text{Co}(\text{en})_3]^{3+}\text{SO}_4^{2-}$ , 18372-71-9;  $[\text{Co}(\text{en})_3]^{3+}$ , 14878-41-2.

(38) The smaller values of  $r_{l(\text{MX})}$  for  $n = 1$  may be partly due to the lability of solvent-separated ion pairs, which may exist in an appreciable proportion because of weaker electrostatic attraction between the anion and the complex ion.

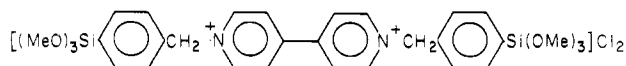
## Synthesis and Characterization of a Benzylviologen Surface-Derivatizing Reagent. *N,N'*-Bis[*p*-(trimethoxysilyl)benzyl]-4,4'-bipyridinium Dichloride

Raymond N. Dominey, Thomas J. Lewis, and Mark S. Wrighton\*

Department of Chemistry, Massachusetts Institute of Technology, Cambridge, Massachusetts 02139 (Received: February 22, 1983)

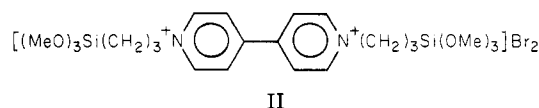
*N,N'*-Bis[*p*-(trimethoxysilyl)benzyl]-4,4'-bipyridinium dichloride, I, can be synthesized by reaction of 4,4'-bipyridine with *p*-(trimethoxysilyl)benzyl chloride in refluxing  $\text{CH}_3\text{CN}$ . Reagent I can be used to functionalize electrode surfaces forming a redox-active polysiloxane,  $[(\text{BPQ}^{2+})_n]_{\text{surf}}$ , via hydrolysis of the Si-OMe bonds. Pt, W, n-Si, and  $\text{SnO}_2$  electrodes derivatized with I have been characterized by electrochemical techniques and surface-sensitive spectroscopies. In aqueous electrolyte the  $E^\circ$  for the  $[(\text{BPQ}^{2+/+})_n]_{\text{surf}}$  system is  $-0.51 \pm 0.05$  V vs. SCE. Both  $[(\text{BPQ}^{2+})_n]_{\text{surf}}$  and  $[(\text{BPQ}^+)_{n-1}]_{\text{surf}}$  are durable when exposed to aqueous electrolyte solution. Further reduction to  $[(\text{BPQ}^0)_{n-2}]_{\text{surf}}$ ,  $E^\circ \approx -0.9$  V vs. SCE, leads to relatively rapid loss of electroactive material. Optical properties of  $\text{SnO}_2/[(\text{BPQ}^{2+/+})_n]_{\text{surf}}$  show that the surface-confined polymer from I is a promising electrochromic material based on the  $[(\text{BPQ}^{2+})_n]_{\text{surf}}(\text{colorless}) \rightleftharpoons [(\text{BPQ}^+)_{n-1}]_{\text{surf}}(\text{blue-violet})$  interconversion. Effective diffusion constants for the  $[(\text{BPQ}^{2+})_n]_{\text{surf}} \rightarrow [(\text{BPQ}^+)_{n-1}]_{\text{surf}}$  process are approximately  $10^{-9}$   $\text{cm}^2/\text{s}$  for a coverage of  $\geq 5 \times 10^{-8}$   $\text{mol}/\text{cm}^2$ . Even at  $10^{-7}$   $\text{mol}/\text{cm}^2$ , greater than 50% reduction of  $[(\text{BPQ}^{2+})_n]_{\text{surf}}$  can be effected in <50 ms. At steady state, >20  $\text{mA}/\text{cm}^2$  can pass through a  $[(\text{BPQ}^{2+/+})_n]_{\text{surf}}$  system at a coverage of  $\sim 3 \times 10^{-8}$   $\text{mol}/\text{cm}^2$ . The  $[(\text{BPQ}^{2+})_n]_{\text{surf}}$  will bind transition-metal complexes in the following ordering of binding strength:  $\text{Mo}(\text{CN})_8^{3-/4-} > \text{Ru}(\text{CN})_6^{3-/4-} > \text{Co}(\text{CN})_6^{3-} > \text{Fe}(\text{CN})_6^{3-/4-} > \text{IrCl}_6^{2-/3-} \gg \text{Cl}^-$ . The bound complexes have nearly the same  $E^\circ$  as when dissolved in solution, consistent with the conclusion that both halves of the redox couple are equally firmly bound.

We wish to report the synthesis of I and the charac-



I

terization of electrode surfaces functionalized with it. The surface-derivatizing reagent I is a derivative of benzylviologen capable of polymerizing via hydrolysis of the  $\text{Si}(\text{OMe})_3$  groups to form a polysiloxane and covalent attachment to surfaces via reaction of surface OH with the  $\text{Si}(\text{OMe})_3$  groups. A closely related benzylviologen derivative<sup>1</sup> and an *N,N'*-dialkyl-4,4'-bipyridinium derivative, II,<sup>2</sup>



II

for derivatizing surfaces have been previously reported. Electrodes derivatized with the viologen reagents<sup>1,2</sup> have been demonstrated to be useful in hydrogen-evolution catalysis on p-type semiconducting photocathodes,<sup>2-6</sup> ca-

(1) Willman, K. W.; Murray, R. W. *J. Electroanal. Chem.* 1982, 133, 211.

(2) Bookbinder, D. C.; Bruce, J. A.; Dominey, R. N.; Lewis, N. S.; Wrighton, M. S. *Proc. Natl. Acad. Sci., U.S.A.* 1980, 77, 6280.

alysis of redox reactions of biological molecules,<sup>7,8</sup> binding of redox-active metal complexes,<sup>9</sup> and electrochromism.<sup>1,10</sup>

We undertook the synthesis and study of I with the expectation that the structural changes in the polysiloxane would result in changes in properties. In the main we find that the properties parallel those previously found for an *N,N'*-dialkyl-4,4'-bipyridinium derivatizing reagent. However, some subtle, but potentially significant, changes in properties attributable to a more rigid polymer structure are found for surfaces derivatized with I. The polymer derived from I is to be denoted  $(BPQ^{2+})_n$  and when bound to a surface is denoted  $[(BPQ^{2+})_n]_{surf}$ . The counterions for the  $BPQ^{2+}$  units are labile; as formed the material is the dichloride, but the ions actually present depend on the electrolyte.

## Experimental Section

**Materials and Solutions. Electrodes.** After the appropriate ohmic contact was made to the back of the electrode material, further electrode fabrication involved attaching the contacted electrode to a coil of Cu wire with Ag epoxy. The Cu wire was then passed through a glass tube and the electrode surface defined by insulating with ordinary epoxy. Single-crystal n-type Si wafers (0.35 mm thick, (111) face exposed) doped with P (resistivity, 3–7  $\Omega$ -cm) were obtained from Monsanto Co., Electronics Division (Palo Alto, CA). Ohmic contact to n-type Si was made with Ga–In eutectic. Electrodes of Pt were made from small sheets (4 mm  $\times$  8 mm) or lengths of wire (0.5 mm in diameter) of the respective metals. W electrodes consisted of a length of wire insulated with heat shrink tubing. Rotating disk electrodes were fashioned by cutting 4-mm circles of Pt sheet which were then contacted with Ag epoxy. These disks were sealed onto the flattened end of 5-mm o.d. glass capillary tubing and the electrode surface defined with ordinary epoxy. Electrical contact to the Ag epoxy was established by using liquid Hg and a Cu wire.  $SnO_2$  (Sb degenerately doped) coated glass ( $\sim$ 3500 Å thick film, resistivity 21–24  $\Omega$ -cm) was generously donated by Corning Glass Works. Electrodes were made by cutting small ( $\sim$ 0.5  $\times$  1.0 cm) rectangular pieces. Ohmic contact was achieved by rubbing Ga–In eutectic on a portion of the  $SnO_2$  surface.

**Chemicals.** Synthesis of I was as follows: Dry 4,4'-bipyridine (1.73 g, 11 mmol) (Aldrich) was added to *p*-(trimethoxysilyl)benzyl chloride (13.3 g, 54 mmol) (PCR Research Chemicals, Inc.) in 150 mL of dry  $CH_3CN$ . The mixture was refluxed for 15 h, cooled to 298 K, and filtered to collect I, a white solid, in 85% isolated yield. The recrystallization of I was accomplished by adding just enough dry  $CH_3OH$  to a mixture of I in dry  $CH_3CN$  causing I to dissolve. The solvent was slowly evaporated by vacuum until very fine needles began to form. The mixture was then allowed to sit for further crystallization. Compound I dissolves in  $CD_3OD$  sufficiently to record the <sup>1</sup>H NMR: ( $CD_3OD$ , 270 MHz)  $\delta$  9.37 (d, 4,  $J$  = 7 Hz), 8.69 (d, 4,  $J$  = 7 Hz), 7.72 (d, 4,  $J$  = 8 Hz), 7.62 (d, 4,  $J$  = 8 Hz), 6.01 (s, 4), 3.59 (s, 18). Anal. (Galbraith) Calcd. (Found):

C, 55.46 (54.78); H, 5.90 (5.93); N, 4.31 (4.33); Si, 8.65 (9.32).

Polarographic-grade  $[n-Bu_4N]ClO_4$  from Southwestern Analytical Chemicals was vacuum dried at 353 K for 24 h and stored in a desiccator until use.  $K_4Ru(CN)_6$  was obtained from Varlacoid Chemical Co. All other chemicals were used as received from the supplier (usually Aldrich, Alfa, or Strem). The  $CH_3CN$  (HPLC grade) was distilled from  $P_2O_5$  before use. If rigorously anhydrous conditions were necessary, the  $CH_3CN/[n-Bu_4N]ClO_4$  electrolyte solution was stored over activated alumina.

**Electrode Derivatization.** Before electrode use or derivatization with I the electrodes were carried through certain pretreatments. Pt electrodes were pretreated as follows: (1) potentiostat at +1.9 V vs. SCE in 0.5 M  $H_2SO_4$  for 5 min; (2) cycle repetitively between –0.1 and +1.0 V vs. SCE for 2–3 h; (3) anodize at +1.1 V vs. SCE for 60 s; (4)  $H_2O$  rinse; and (5) air-dry. The optically transparent  $SnO_2$  electrodes were pretreated by a 60-s soak in 10 M NaOH followed by rinsing with distilled  $H_2O$  and air-drying. For n-type Si the pretreatment was to etch in concentrated HF for 30–60 s and then rinse with distilled  $H_2O$ . The Si electrodes were then immersed in 10 M NaOH for 60 s, washed with  $H_2O$  followed by acetone, and then air-dried. The W electrodes were typically pretreated by sanding to expose fresh W followed by a 5-s dip in concentrated  $HNO_3$ .

After pretreatment, functionalization with I was effected by soaking the pretreated electrode in a 2–5 mM solution of I in  $\sim$ 2%  $CH_3OH/CH_3CN$  (by volume) for 1–7 days. Addition of 1–10 drops of pH 3.5  $H_2O$  (acidified with HCl) was often made to speed polymerization. For Pt and  $SnO_2$  derivatization with I was usually achieved by potentiostating the pretreated electrode at –0.64 V vs. SCE in nonstirred aqueous 0.1 M  $K_2HPO_4/0.2$  M KCl/ $\sim$ 0.5 mM I under Ar for 0.5–2 h. Coverage of  $[(BPQ^{2+})_n]_{surf}$  was determined by integration of the cathodic peak of the cyclic voltammogram for  $[(BPQ^{2+})_n]_{surf} \rightleftharpoons [(BPQ^+)_n]_{surf}$  at a sweep sufficiently slow ( $\leq$ 100 mV/s) to completely reduce the  $[(BPQ^{2+})_n]_{surf}$ .

**General Procedures. Electrochemistry.** Cyclic voltammetry and steady-state current–voltage data were obtained by using a PAR Model 173 potentiostat equipped with a Model 179 digital coulometer and a Model 175 voltage programmer. Data were recorded on a Houston Instruments X–Y recorder. All electrochemistry was carried out by using rigorously deoxygenated media, since the reduced viologens are  $O_2$  sensitive. Experiments in  $H_2O$  solution were performed in a single-compartment Pyrex cell with a saturated calomel reference electrode (SCE), Pt counterelectrode, and the appropriate working electrode. Experiments in  $CH_3CN$  solution utilized a Ag/Ag<sup>+</sup>  $CH_3CN$  reference electrode at +0.35 V vs. SCE.

For the potential step chronoamperometry, data were recorded on a Tektronix Model 564B storage oscilloscope. The spectroelectrochemical experiments were performed by using an electrochemical cell fitted with quartz windows and placed in the sample chamber of a Cary 17 UV–vis–near-IR spectrometer.

For rotating disk electrode experiments, the finished electrodes were mounted in the shaft of a variable-speed stirring motor from Polysciences, Inc. Speeds from 200 to 2400 rpm can be obtained. The actual speed was established by calibrating the motor settings with a photodiode connected to a tachometer (Power Instruments, Inc., Skokie, IL). These readings were also checked by monitoring the response of a photodiode to an irradiated reflector mounted concentrically on the disk shaft using a calibrated oscilloscope to measure the photodiode output.

(3) Abruna, H. D.; Bard, A. J. *J. Am. Chem. Soc.* 1981, 103, 6898.

(4) Bruce, J. A.; Murahashi, T.; Wrighton, M. S. *J. Phys. Chem.* 1982, 86, 1552.

(5) Bruce, J. A.; Wrighton, M. S. *Isr. J. Chem.* 1982, 22, 184.

(6) Dominey, R. N.; Lewis, N. S.; Bruce, J. A.; Bookbinder, D. C.; Wrighton, M. S. *J. Am. Chem. Soc.* 1982, 104, 467.

(7) Lewis, N. S.; Wrighton, M. S. *Science* 1981, 211, 944.

(8) Bookbinder, D. C.; Lewis, N. S.; Wrighton, M. S. *J. Am. Chem. Soc.* 1981, 103, 7656.

(9) Bruce, J. A.; Wrighton, M. S. *J. Am. Chem. Soc.* 1982, 104, 74.

(10) Bookbinder, D. C.; Wrighton, M. S. *J. Electrochem. Soc.* 1983, 130, 1080.

The Pt rotating disk electrodes were checked by monitoring the current,  $i$ , vs.  $\omega^{1/2}$ , (rotation velocity) $^{1/2}$ , at +0.7 V vs. SCE for the oxidation of 4 mM  $\text{Fe}(\text{CN})_6^{4-}$  in 2 M KCl. The test redox couple,  $\text{Fe}(\text{CN})_6^{3-/4-}$ , was chosen for convenience and its fast heterogeneous electron-transfer kinetics. Plots of  $i$  vs.  $\omega^{1/2}$  are linear up to the highest rotation velocity (at 2400 rpm) for acceptable electrodes.<sup>11</sup>

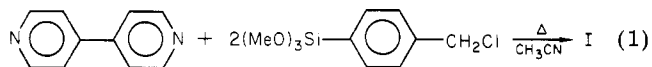
Anion-exchange experiments with the  $[(\text{BPQ}^{2+})_n]_{\text{surf}}$  systems were performed by placing the electrode into an aqueous solution containing the appropriate ions. The electrode was then left to equilibrate without potentiostatic control. Electrochemical detection of the anions was accomplished by cyclic voltammetry or by transmission IR for n-Si/ $[(\text{BPQ}^{2+})_n]_{\text{surf}}$  electrodes.

**Auger Spectroscopy and Scanning Electron Microscopy.** Auger spectra and depth profiles were obtained with a Physical Electronics Model 590A scanning Auger spectrometer. Scanning electron microscopy and X-ray spectrometry were taken on a Cambridge Mark 2A Stereoscan equipped with a Kevex energy dispersive X-ray analyzer.

**Fourier Transform Infrared Spectroscopy.** Infrared spectral data were taken with a Nicolet 7199 Fourier transform spectrometer. The n-type Si substrate was cut from wafers to give flag electrodes of  $\sim 1.2 \text{ cm} \times 1.5 \text{ cm}$ . The ohmic contact was made on a strip at the top of one side. To minimize  $\text{H}_2\text{O}$  interference, the electrodes were usually enclosed in a Schlenk tube after the particular treatment was finished and the tube evacuated for 2–3 h. Additionally, the spectrometer chamber was purged with liquid- $\text{N}_2$  boil-off for at least 30 min prior to running spectra. Typically, 576 scans were collected at a resolution of  $4 \text{ cm}^{-1}$  before transforming.

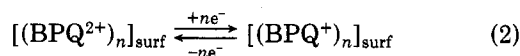
## Results

**Synthesis of I.** Reagent I can be synthesized quickly and cleanly according to eq 1. The desired product pre-



cipitates from solution and can be collected in a pure state by filtration. Since benzyl chloride is more reactive than *n*-propyl bromide, the synthesis of I can be effected more rapidly than for II, under a given set of conditions.

**Electrochemistry of Electrodes Derivatized with I.** After appropriate pretreatment, electrode surfaces can be derivatized with I by either soaking in a 2–5 mM solution of I in  $\text{CH}_3\text{CN}/\text{CH}_3\text{OH}$  or by potentiostating the pretreated electrodes at  $-0.64 \text{ V}$  vs. SCE in a  $\sim 0.5 \text{ mM}$  solution of I in aqueous 0.2 M KCl/0.1 M  $\text{K}_2\text{HPO}_4$  (see Experimental Section). Like electrodes derivatized with II, electrodes derivatized with I show a persistent electrochemical response in aqueous electrolyte solution. The cyclic voltammetry as a function of sweep rate for a derivatized Pt electrode in aqueous electrolyte solution is shown in Figure 1; the wave at  $\sim -0.5 \text{ V}$  vs. SCE is attributable to the process represented by eq 2. The in-



terconversion represented by eq 2 has been effected  $>25\,000$  times without significant loss of electroactive material. Further, electrodes derivatized with I can be held at  $E^\circ[(\text{BPQ}^{2+/+})_n]_{\text{surf}}$  for prolonged periods of time (at least 12 h) in deoxygenated aqueous electrolyte solutions without deterioration in properties. Exposure of

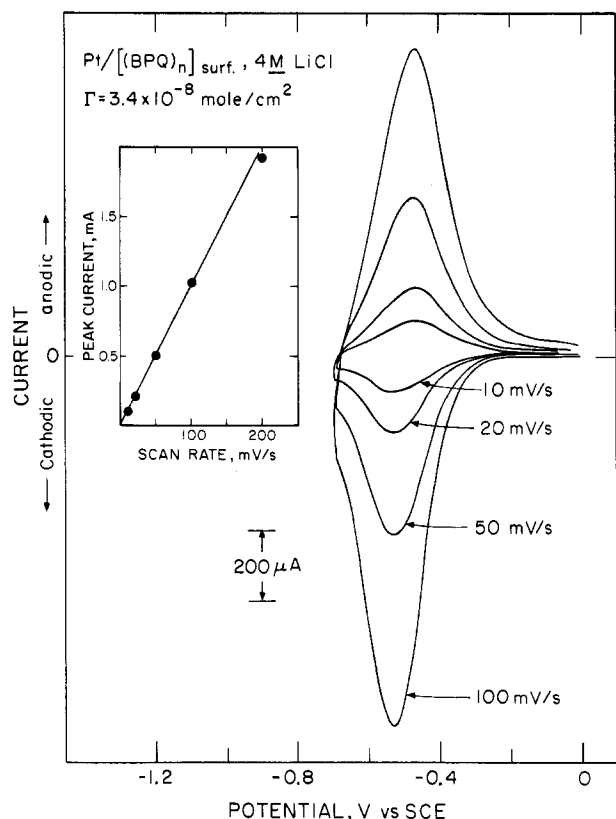
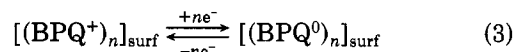


Figure 1. Cyclic voltammetry for Pt/ $[(\text{BPQ}^{2+})_n]_{\text{surf}}$  in aqueous electrolyte as a function of sweep rate.

$[(\text{BPQ}^+)_{n}]_{\text{surf}}$  to  $\text{O}_2$  leads to rapid loss of electroactive material, in accord with the known sensitivity of reduced viologens to  $\text{O}_2$ .<sup>12</sup> A second cyclic voltammetry wave is observed at  $\sim -0.9 \text{ V}$  vs. SCE when  $\text{H}_2$  evolution is unimportant as on  $\text{SnO}_2$  or when  $\text{CH}_3\text{CN}$  is added to the aqueous electrolyte in the case of Pt electrodes. The second wave is associated with the process represented by eq 3. While the doubly reduced viologen species are



generally not durable in aqueous media, we find that good cyclic voltammograms can be obtained for the first and second reduction of  $[(\text{BPQ}^{2+})_n]_{\text{surf}}$  in aqueous KCl or LiCl. The potentials from the cyclic voltammetry waves are within 100 mV of the values for benzylviologen in solution.<sup>13</sup> Generally, reversible, one-electron couples anchored to surfaces have an  $E^\circ$  with 100 mV of the solution analogue.<sup>14</sup> The charge associated with both waves for surfaces derivatized with I is the same. These facts are all consistent with surface attachment of intact benzylviologen units. However, potential excursions to form  $[(\text{BPQ}^0)_{n}]_{\text{surf}}$  lead to relatively rapid loss of electroactive material. Figure 2 shows the loss in cyclic voltammetry signal upon scanning to the two-electron reduced state for both the polymer from I and the polymer from II. There is no difference in the decay rates of the two systems when the polymer is held in the two-electron reduced state.

The measurement of charge associated with the  $[(\text{BPQ}^{2+})_n]_{\text{surf}} \rightarrow [(\text{BPQ}^+)_{n}]_{\text{surf}}$  reduction to determine

(12) Nanni, E. J., Jr.; Angelis, C. T.; Dickson, J.; Sawyer, D. T. *J. Am. Chem. Soc.* 1981, 103, 4268.

(13) Steckhan, E.; Kuwana, T. *Ber. Bunsenges. Phys. Chem.* 1974, 78, 253.

(14) (a) Murray, R. W. *Acc. Chem. Res.* 1980, 13, 135. (b) Lenhard, J. R.; Rocklin, R.; Abruna, H.; Willman, K.; Kuo, K.; Kowak, R.; Murray, R. W. *J. Am. Chem. Soc.* 1978, 100, 5213.

(11) Bard, A. J.; Faulkner, L. R. "Electrochemical Methods: Fundamentals and Applications"; Wiley: New York, 1980; p 288.

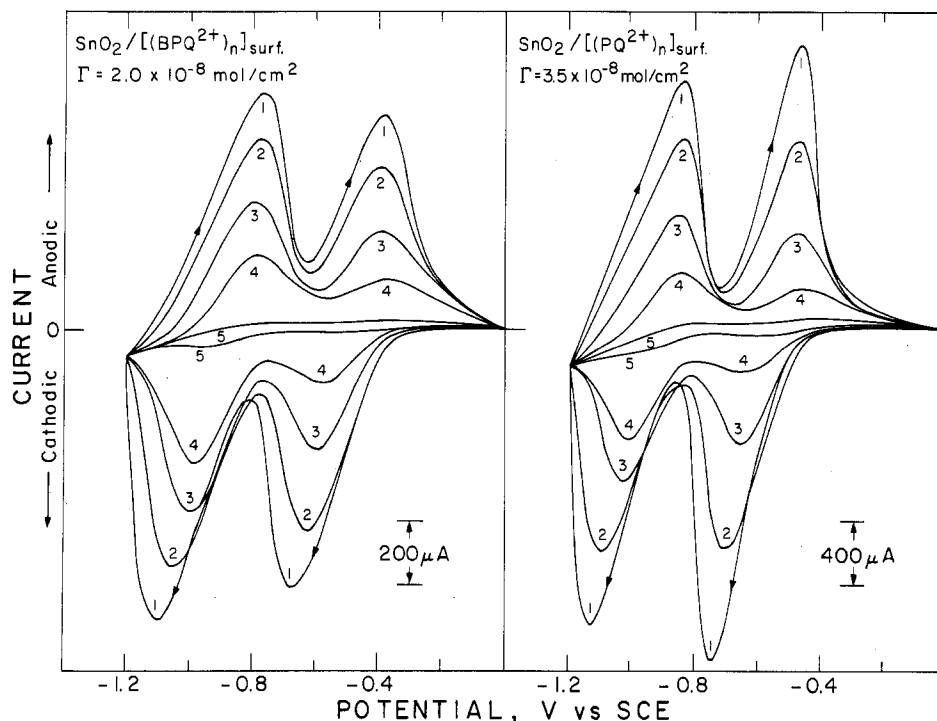


**Figure 2.** Cyclic voltammograms (100 mV/s) of Pt/[BPQ<sup>2+</sup>]<sub>n</sub> and Pt/[PQ<sup>2+</sup>]<sub>n</sub> electrodes in 4.0 M LiCl. The cyclic voltammograms were recorded after each electrode was potentiostated at -1.15 V vs. SCE for (1) 0, (2) 10, (3) 30, (4) 60, and (5) 150 min. The smaller area under the curves is associated with irreversible decomposition associated with reaction of [(BPQ<sup>0</sup>)<sub>n</sub>]<sub>surf</sub>. Pt/[BPQ<sup>2+</sup>]<sub>n</sub> electrodes potentiostated at -0.55 V vs. SCE does not yield loss of electroactive material.

**TABLE I:** Representative Cyclic Voltammetric Data for M/[(BPQ<sup>2+</sup>)<sub>n</sub>]<sub>surf</sub> Electrodes in Aqueous Solution<sup>a</sup>

electrode	medium	Γ, mol/cm <sup>2</sup>	[(BPQ <sup>2+/+</sup> ) <sub>n</sub> ] <sub>surf</sub>			[(BPQ <sup>0</sup> ) <sub>n</sub> ] <sub>surf</sub>		
			E <sub>PC</sub> <sup>b</sup>	E <sup>0'</sup> <sup>c</sup>	E <sub>PA</sub> <sup>b</sup>	E <sub>PC</sub> <sup>b</sup>	E <sup>0'</sup> <sup>c</sup>	E <sub>PA</sub> <sup>b</sup>
Pt no. 1	0.1 M KCl(aq)	3.8 × 10 <sup>-8</sup>	-0.54	-0.49	-0.43			
	4.0 M KCl(aq)		-0.58	-0.55	-0.52			
Pt no. 2	0.1 M KCl(aq)	3.0 × 10 <sup>-8</sup>	-0.53	-0.48	-0.43			
Pt no. 2	4.0 M KCl(aq)		-0.59	-0.56	-0.53			
Pt no. 3	0.1 M KCl(aq)	9.1 × 10 <sup>-8</sup>	-0.59	-0.49	-0.39			
Pt no. 3	1.0 M KCl(aq)		-0.58	-0.54	-0.50			
	4.0 M KCl(aq)		-0.60	-0.57	-0.54			
Pt no. 4	0.2 M KCl(aq)	2.0 × 10 <sup>-8</sup>	-0.53	-0.48	-0.43			
Pt no. 4	0.5 M KI(aq)		-0.53	-0.49	-0.45			
Pt no. 5	1.0 M KCl(aq)	8.6 × 10 <sup>-8</sup>	-0.55	-0.50	-0.46			
Pt no. 6	1.0 M KCl(aq)	7.9 × 10 <sup>-9</sup>	-0.55	-0.49	-0.43			
Pt no. 7	1.0 M KCl(aq)	3.7 × 10 <sup>-9</sup>	-0.54	-0.50	-0.46			
W no. 1	1.0 M KCl(aq)	3.9 × 10 <sup>-8</sup>	-0.62	-0.55	-0.48			
	1.0 M KCl (pH 7) <sup>d</sup>		-0.60	-0.54	-0.48			
	1.0 M KCl (pH 4) <sup>e</sup>		-0.60	-0.54	-0.48			
	1.0 M KCl (pH 1) <sup>f</sup>		-0.59	-0.53	-0.47			
SnO <sub>2</sub> no. 1	1 M KCl (pH 6.8) <sup>d</sup>	2.2 × 10 <sup>-8</sup>	-0.54	-0.51	-0.47	-0.96	-0.90	-0.84
SnO <sub>2</sub> no. 2	1 M KCl (pH 6.8) <sup>d</sup>	5.3 × 10 <sup>-8</sup>	-0.58	-0.52	-0.46	-0.98	-0.91	-0.84
Pt no. 8	0.2 M LiCl, CH <sub>3</sub> CN/H <sub>2</sub> O (50/50)	1.1 × 10 <sup>-7</sup>	-0.50	-0.45	-0.40	-0.86	-0.81	-0.76
Pt no. 9	1.0 M KCl, CH <sub>3</sub> CN/H <sub>2</sub> O (1/100)	1.0 × 10 <sup>-7</sup>	-0.56	-0.50	-0.44	-0.92	-0.86	-0.80
W no. 2	4.0 M LiCl(aq)	2.5 × 10 <sup>-8</sup>	-0.53	-0.49	-0.46	-1.01 <sup>g</sup>	-0.95 <sup>g</sup>	-0.88 <sup>g</sup>

<sup>a</sup> Scan rate is 100 mV/s. <sup>b</sup> E<sub>PC</sub> and E<sub>PA</sub> refer to cathodic and anodic peak potentials, respectively, V vs. SCE. <sup>c</sup> E<sup>0'</sup> is taken to be the average of E<sub>PC</sub> and E<sub>PA</sub>. <sup>d</sup> Phosphate buffer. <sup>e</sup> Acetate buffer. <sup>f</sup> Adjusted to pH 1 with HCl. <sup>g</sup> Significant H<sub>2</sub> evolution current observed.

coverage of BPQ<sup>2+</sup> units has been made at a sweep rate (≤100 mV/s) where the peak current is proportional to sweep rate. Typical coverage of the polymer is >3 × 10<sup>-9</sup> mol of monomer units per cm<sup>2</sup> of geometrical electrode area. Coverages as high as 1.8 × 10<sup>-7</sup> mol/cm<sup>2</sup> have been studied. A coverage of ~10<sup>-10</sup> mol/cm<sup>2</sup> would correspond to an approximate monolayer. Thus, the large coverages measured establish that reagent I can form surface-bound polymers. Table I summarizes some electrochemical data for a variety of electrodes derivatized with I.

In contrast to electrodes derivatized with reagent II, electrodes derivatized with I generally require a substantial

"break-in" period in aqueous electrolyte solution. The break-in can consist of repeated cyclic voltammograms or soaking in 1.0 M KCl for >1 h. During the break-in period the apparent coverage of (BPQ<sup>2+</sup>)<sub>n</sub> grows and the cyclic voltammetry waves become sharper. The behavior of electrodes derivatized with I in CH<sub>3</sub>CN/0.1 M [n-Bu<sub>4</sub>N]ClO<sub>4</sub> also differs from electrodes functionalized with II: significantly less apparent electroactive material is detected by cyclic voltammetry compared to the amount of detected material in H<sub>2</sub>O/electrolyte. These differences between reagents I and II are attributable to differences in the nature of polysiloxanes that result from these two

TABLE II: Diffusion Coefficients Obtained from Cottrell Plots for Pt/[(BPQ<sup>2+</sup>)<sub>n</sub>]<sub>surf</sub><sup>a</sup>

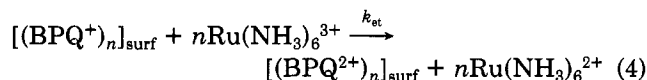
$\Gamma$ , mol/cm <sup>2</sup>	electrolyte	potential step, V vs. SCE	10 <sup>9</sup> D, cm <sup>2</sup> /s
9.0 × 10 <sup>-8</sup>	0.1 M KCl	0.0 → -0.65	0.58
	1.0 M KCl	0.0 → -0.65	2.2
	4.0 M KCl	0.0 → -0.65	4.1
3.2 × 10 <sup>-8</sup>	1.0 M KCl	0.0 → -0.64	2.6
	4.0 M LiCl	0.0 → -0.65	3.3

<sup>a</sup> Obtained from plots of  $i$  vs.  $t^{-1/2}$ . Data are for the [(BPQ<sup>2+</sup>)<sub>n</sub>]<sub>surf</sub> → [(BPQ<sup>+</sup>)<sub>n</sub>]<sub>surf</sub> process. The concentration of BPQ<sup>2+</sup> is taken to be 2.2 M for use in calculating  $D$  from the slope of the  $i$  vs.  $t^{-1/2}$  plots.

molecules. The data in Table I show that the cyclic voltammetry of [(BPQ<sup>2+</sup>)<sub>n</sub>]<sub>surf</sub> at 100 mV/s is even affected by the KCl concentration. At the higher KCl concentration the waves in a cyclic voltammogram are sharper and somewhat more negative than at the lower concentration. As the data for W/[(BPQ<sup>2+</sup>)<sub>n</sub>]<sub>surf</sub> show, the  $E^{\circ'}$  is independent of pH in the range pH 1–7.

From cyclic voltammograms it is apparent that the [(BPQ<sup>2+</sup>)<sub>n</sub>]<sub>surf</sub> can be rapidly reduced. Indeed, it would appear that the peak current is directly proportional to sweep rate up to ~200 mV/s. This suggests that the kinetics for the reduction of the polymer are good. At higher sweep rates, though, the reduction appears to be limited by some sort of diffusion process. Potential step chronoamperometry experiments have been carried out and show that a potential step from 0.00 to -0.65 V vs. SCE results in a current,  $i$ , that is proportional to  $t^{-1/2}$  for a significant time period for coverages of (BPQ<sup>2+</sup>)<sub>n</sub> > 3 × 10<sup>-8</sup>. These data are consistent with a diffusion-limited reduction where the Cottrell equation<sup>15</sup> can be used to determine an effective diffusion constant,  $D$ , as has been done for other surface-confined polymers.<sup>16</sup> Values of  $D$  of ~4 × 10<sup>-9</sup> cm<sup>2</sup>/s have been obtained for coverages of 10<sup>-8</sup>–10<sup>-7</sup> mol/cm<sup>2</sup> in 4.0 M KCl (Table II). In some cases the Cottrell plots are not linear and reflect problems with film resistance that have been noticed in other cases.<sup>16</sup> In practical terms, we find the [(BPQ<sup>2+</sup>)<sub>n</sub>]<sub>surf</sub> can be reduced by >50% in less than 50 ms for a potential step from 0.00 to -0.65 V vs. SCE in 4.0 M KCl for coverages of ≤10<sup>-7</sup> mol/cm<sup>2</sup>. These data are qualitatively the same as obtained for electrodes derivatized with II.<sup>10</sup> The values of  $D$  for electrodes derivatized with I, however, are significantly larger than previously reported for a benzylviologen-based polymer.<sup>1</sup>

Another important aspect of the electrochemical properties of a surface-confined polymer is the steady-state current that can pass through the polymer. In order to probe this aspect of the [(BPQ<sup>2+</sup>)<sub>n</sub>]<sub>surf</sub> system we have studied the reduction of Ru(NH<sub>3</sub>)<sub>6</sub><sup>3+</sup> at Pt/[(BPQ<sup>2+</sup>)<sub>n</sub>]<sub>surf</sub> rotating disk electrodes (Figures 3 and 4). The (BPQ<sup>2+</sup>)<sub>n</sub> coverage used was sufficiently uniform and large to ensure that the reduction proceeds via 4, not via a direct reduction



at the Pt surface through gross pinholes in the polymer or by diffusion of Ru(NH<sub>3</sub>)<sub>6</sub><sup>3+</sup> through the polymer. That the direct reduction on the Pt does not occur is evidenced by the fact that the reduction current for the production of Ru(NH<sub>3</sub>)<sub>6</sub><sup>2+</sup> onsets at the potential corresponding to the onset for the reduction of [(BPQ<sup>2+</sup>)<sub>n</sub>]<sub>surf</sub> and does not onset

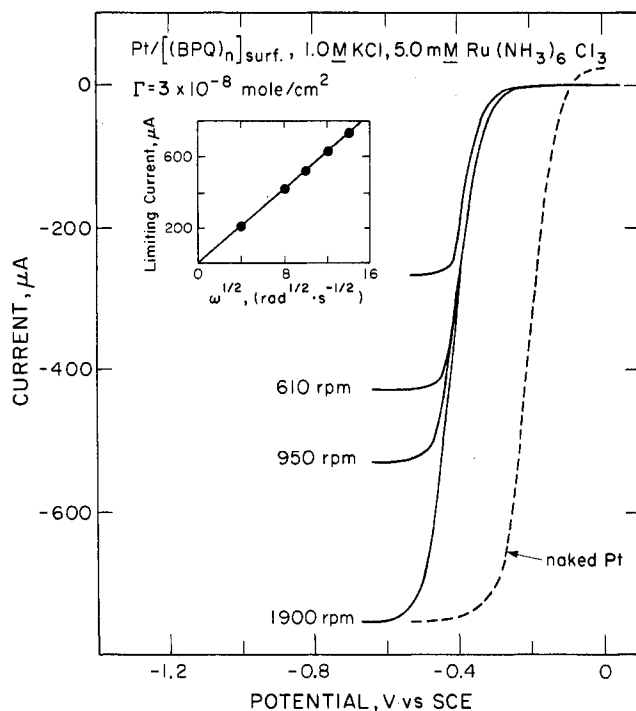


Figure 3. Steady-state current-voltage curves (1 mV/s) for a rotated Pt disk electrode (diameter, 0.55 cm), naked (---), and derivatized (—), with I, ~3 × 10<sup>-8</sup> mol/cm<sup>2</sup>, in aqueous 1.0 M KCl containing 5.0 mM Ru(NH<sub>3</sub>)<sub>6</sub>Cl<sub>3</sub>. Limiting current at -0.62 V vs. SCE is shown (inset) to be linear with (rotation velocity)<sup>1/2</sup>.

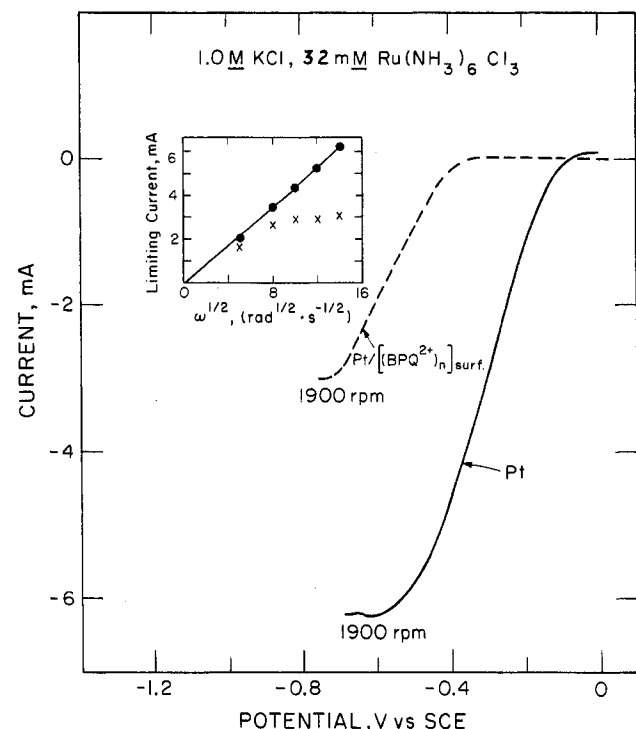
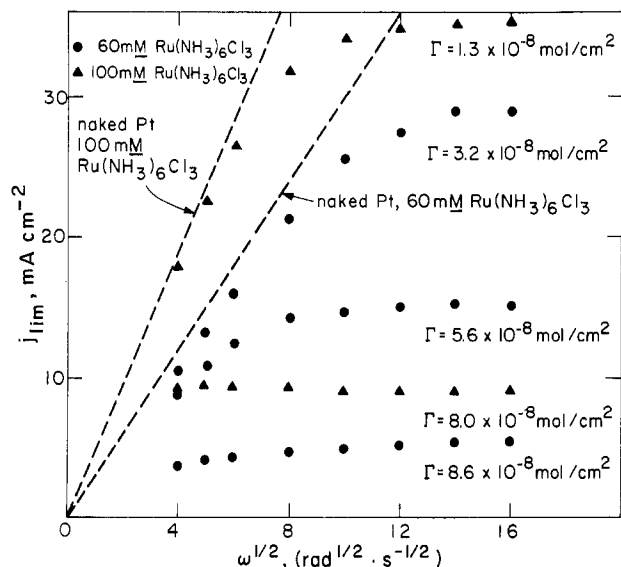


Figure 4. As in Figure 3 except for 32 mM Ru(NH<sub>3</sub>)<sub>6</sub>Cl<sub>3</sub>. Inset shows a linear plot of limiting current vs. (rotation velocity)<sup>1/2</sup> for the naked Pt (●) where the limiting current from the derivatized electrode levels off at  $\omega^{1/2} \geq 8$ .

at the potential characteristic of naked Pt (Figures 3 and 4). The data in Figure 3 for 5 mM Ru(NH<sub>3</sub>)<sub>6</sub><sup>3+</sup> show that, when the surface-bound material from I is in the (BPQ<sup>+</sup>)<sub>n</sub> form, the only limitation to the rate of formation of Ru(NH<sub>3</sub>)<sub>6</sub><sup>2+</sup> is mass transport of Ru(NH<sub>3</sub>)<sub>6</sub><sup>3+</sup> up to the surface of the electrode, up to the highest rotation speed. This conclusion follows from the strict linearity of the plot of

(15) Bard, A. J.; Faulkner, L. R. "Electrochemical Methods: Fundamentals and Applications"; Wiley: New York, 1980; p 143.

(16) Daum, P.; Murray, R. W. *J. Phys. Chem.* 1981, 85, 389.



**Figure 5.** Representative Levich plots for the reduction of 60 and 100 mM  $\text{Ru}(\text{NH}_3)_6\text{Cl}_3$  at rotating  $\text{Pt}/[(\text{BPQ}^{2+})_n]_{\text{surf}}$  electrodes in 1.0 M LiCl electrolyte solution. The dashed lines are the responses obtained at naked platinum electrodes.

limiting current vs.  $\omega^{1/2}$ .<sup>11</sup> In this case the reduction of the  $\text{Ru}(\text{NH}_3)_6^{3+}$  must be occurring at the outermost surface of the polymer. The steady-state current passing through the polymer can thus be  $>4 \text{ mA}/\text{cm}^2$ ; i.e., at steady-state the rate of charge transport through the  $[(\text{BPQ}^{2+/+})_n]_{\text{surf}}$  can exceed  $4 \text{ mA}/\text{cm}^2$  via a self-exchange charge transport mechanism involving the  $\text{BPQ}^{2+/+}$  units. A plot of the limiting current vs.  $\omega^{1/2}$  is linear for low  $\text{Ru}(\text{NH}_3)_6^{3+}$  concentrations when the electrode is held at a potential where the surface polymer is in the  $[(\text{BPQ}^+)_n]_{\text{surf}}$  state. This establishes that  $k_{\text{et}}$  is at least  $\sim 10^6 \text{ M}^{-1} \text{ s}^{-1}$ .

At higher concentrations of  $\text{Ru}(\text{NH}_3)_6^{3+}$  the plot of limiting current vs.  $\omega^{1/2}$  is distinctly nonlinear and the current clearly becomes limited by something other than mass transport of  $\text{Ru}(\text{NH}_3)_6^{3+}$  up to the  $\text{Pt}/[(\text{BPQ}^{2+})_n]_{\text{surf}}$  electrode (Figures 4 and 5). The current limitation must be due to the slow charge transport through the polymer. The value of  $k_{\text{et}}$  should not be limiting, since the plots should be nonlinear at low, not high, concentrations of  $\text{Ru}(\text{NH}_3)_6^{3+}$ . Since the rate of reducing high concentrations of  $\text{Ru}(\text{NH}_3)_6^{3+}$  can be completely limited by the rate of charge transport through the  $[(\text{BPQ}^{2+/+})_n]_{\text{surf}}$ , the limiting current would then be a function of the thickness of the polymer. Data in Figure 6 show that the limiting current corresponding to the reduction of 60 or 100 mM  $\text{Ru}(\text{NH}_3)_6^{3+}$  according to eq 4 is inversely proportional to coverage of  $[(\text{BPQ}^{2+/+})_n]$  in the range of coverages investigated. Interestingly, the charge transport through the polymer would appear to be sufficient to offer negligible limitation to solar energy conversion efficiency for photoelectrodes modified with I at a coverage ( $1 \times 10^{-8} \text{ mol}/\text{cm}^2$ ) where a uniform film of the polymer would be expected. A similar conclusion can be drawn for electrodes derivatized with II.

**Optical Properties of  $[(\text{BPQ}^{2+/+})_n]_{\text{surf}}$ .** The reduction of  $[(\text{BPQ}^{2+})_n]_{\text{surf}}$  is accompanied by large optical spectral changes (Figure 7). Colorless films of  $[(\text{BPQ}^{2+})_n]_{\text{surf}}$  become blue upon reduction to  $[(\text{BPQ}^+)_n]_{\text{surf}}$  and then golden yellow upon further reduction to  $[(\text{BPQ}^0)_n]_{\text{surf}}$ . The color changes are easily detectable to the naked eye for coverages of  $>1 \times 10^{-8} \text{ mol}/\text{cm}^2$ . Interestingly, the  $[(\text{BPQ}^+)_n]_{\text{surf}}$  is blue, whereas electrodes derivatized with II become purple upon one-electron reduction.<sup>10</sup> The absorption maximum for  $[(\text{BPQ}^+)_n]_{\text{surf}}$  is 610 nm, compared to the 545 nm for

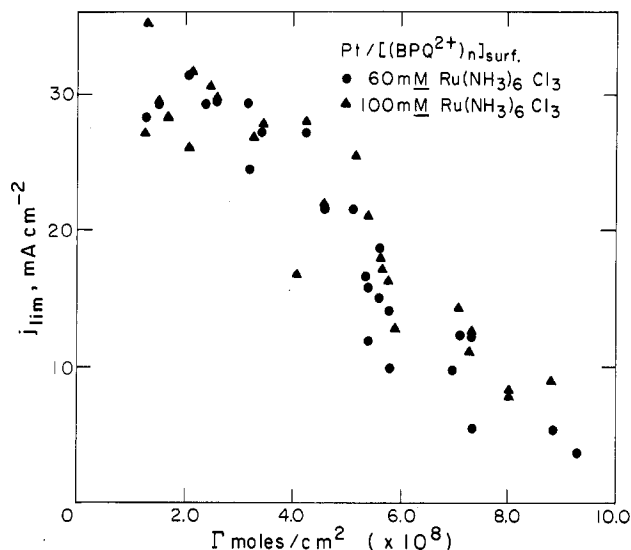


**Figure 6.** Limiting current as a function of coverage of  $(\text{BPQ}^{2+})_n$  for the reduction of 60 and 100 mM  $\text{Ru}(\text{NH}_3)_6\text{Cl}_3$  in 1.0 M LiCl.

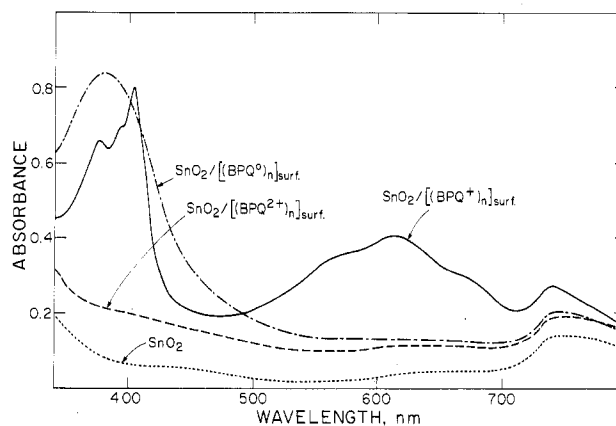


**Figure 7.** Absorption spectra of "naked"  $\text{SnO}_2$  (---) and of the  $\text{SnO}_2/[(\text{BPQ}^{2+/1+/0})_n]_{\text{surf}}$  redox system in 1 M KCl. The spectrum of  $[(\text{BPQ}^{2+})_n]_{\text{surf}}$  (---) was taken with the electrode potentiostated at 0.0 V vs. SCE. The spectrum of  $[(\text{BPQ}^+)_n]_{\text{surf}}$  was taken with the electrode potentiostated at  $-0.68 \text{ V}$  vs. SCE. The spectrum of  $[(\text{BPQ}^0)_n]_{\text{surf}}$  was taken with the electrode potentiostated at  $-1.2 \text{ V}$  vs. SCE.

the one-electron reduced polymer derived from II. A further noteworthy feature is that, when derivatization with I is effected by potentiostating an electrode to "electroplate"  $[(\text{BPQ}^+)_n]_{\text{surf}}$ , the film is initially distinctly purple. However, after break-in the  $[(\text{BPQ}^+)_n]_{\text{surf}}$  is blue in appearance. The purple color of the deposited material from I is attributable to aggregation<sup>17</sup> believed to be responsible for the purple color of the polymer from II.<sup>10</sup> While dilute solutions of the one-electron reduced  $N,N'$ -dialkyl-4,4'-bipyridinium are blue, higher concentrations produce aggregates that are purple.<sup>10,17</sup> The blue color of the  $[(\text{BPQ}^+)_n]_{\text{surf}}$  suggests that the polymer structure is sufficiently rigid to prevent the interaction between the  $\text{BPQ}^+$  units that gives the spectral change from blue to purple in appearance.

The purple color for material derived from II has been associated with an  $E^{\circ'}$  that is shifted to a more positive potential compared to the  $E^{\circ'}$  for the solution species. Benzylviologen has an  $E^{\circ'}$  that is somewhat more positive than the alkylviologen,<sup>13</sup> but attachment of I gives an  $E^{\circ'}$  that is shifted less than the shift accompanying attachment

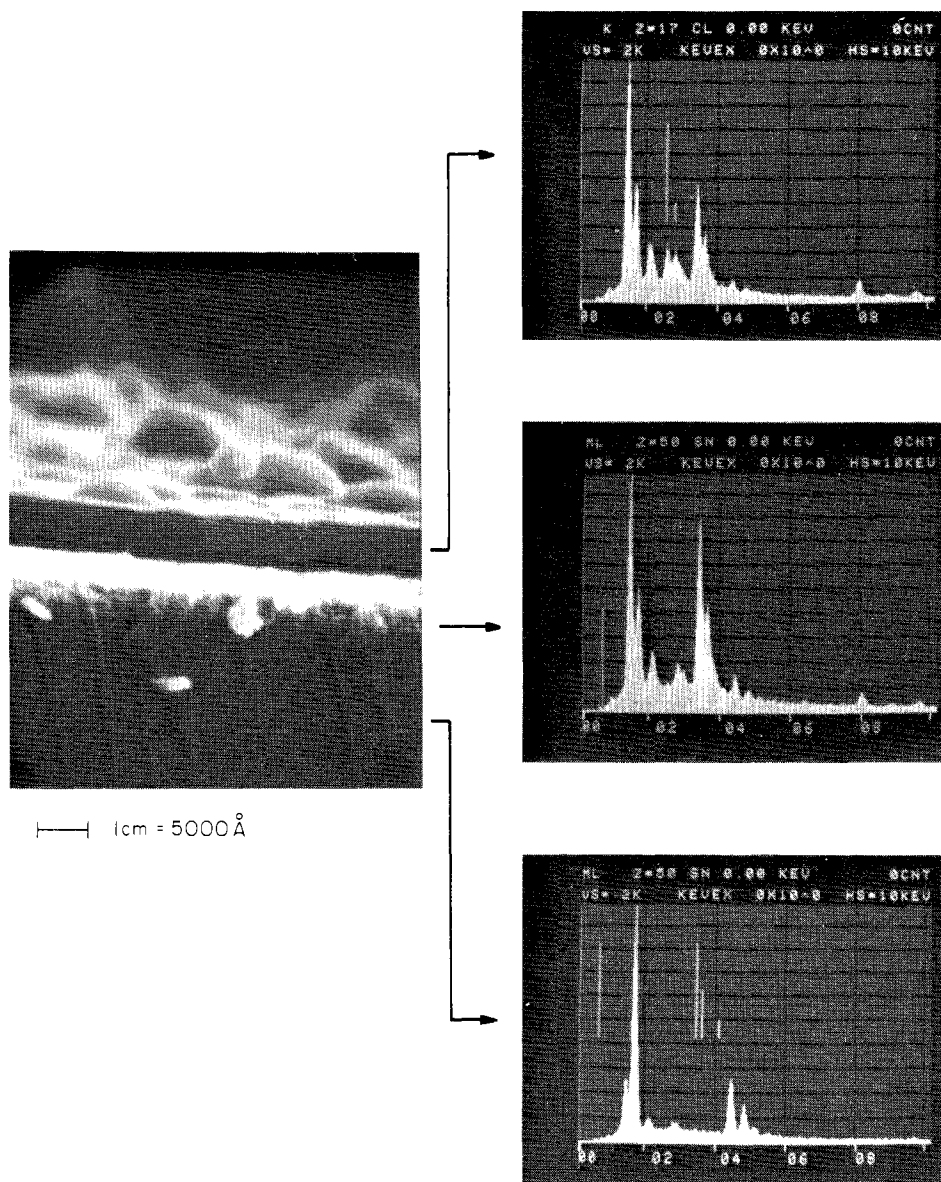
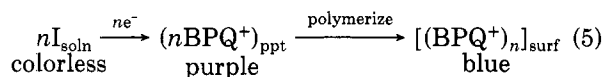


**Figure 8.** Scanning electron micrograph (left) of the edge of a  $\text{SnO}_2$  electrode (thin film on glass substrate) which has been derivatized with I (coverage  $> 10^{-7}$  mol/cm $^2$ ) at a  $2.0 \times 10^4$  magnification. The accompanying pictures (to the right) are energy dispersive X-ray analyses of the three different layers: (from top to bottom) the  $[(\text{BPQ}^{2+})_n \cdot 2n\text{Cl}^-]_{\text{surf}}$  layer; the  $\text{SnO}_2$  layer; and the glass substrate. The marker bars in the top show the expected position of Cl signals; marker bars in the middle and bottom depict the expected position of Sn signals. The bottom X-ray shows signals due to Si of the glass.

of II.<sup>2-6</sup> In the electroplating of I (to give an initially purple colored material) there is a cyclic voltammetry wave at a more positive position,  $\sim -0.4$  V vs. SCE, than that ultimately observed for  $[(\text{BPQ}^{2+/+})_n]_{\text{surf}}$ . The optical and electrochemical results are consistent with a sequence as in eq 5 upon potentiostatic deposition of I onto electrodes



where there is an initial electrochemical precipitation of I onto the electrode as a purple aggregate of the one-electron reduced material. The aggregate can then polymerize via hydrolysis of the  $\text{Si}(\text{OMe})_3$  groups to form  $[(\text{BPQ}^+)_n]_{\text{surf}}$ .

The absorptivity of the  $[(\text{BPQ}^+)_n]_{\text{surf}}$  has been determined. Data for the 610-nm maximum show that the absorptivity is  $\sim 1 \times 10^7$  cm $^2$ /mol or  $10^4$  M $^{-1}$  cm $^{-1}$ , in accord with the absorptivity for the one-electron reduced state of benzylviologen in solution.<sup>13</sup> Table III gives some representative data.

**TABLE III:** Optical Spectroscopic and Scanning Electron Microscopic Measurements for the  $\text{SnO}_2/[(\text{BPQ}^{2+})_n]_{\text{surf}}$  System

elec- trode	$10^8 \Gamma$ , <sup>a</sup> mol/cm $^2$	OD at 610 nm <sup>b</sup>	film thickness, <sup>c</sup> Å	$10^{-3} \epsilon_{610\text{nm}}$ , <sup>d</sup> cm $^2$ /mol
1	2.4	0.22	930	9 200
2	2.2	0.22	1130	10 000
3	3.2	0.40	1630	12 500
4	3.3	0.37	1600	11 200

<sup>a</sup> The coverages were determined by integration of a cyclic voltammogram. <sup>b</sup> Measured at  $-0.6$  V vs. SCE in 0.1 M KCl to generate  $[(\text{BPQ}^+)_n]_{\text{surf}}$ . <sup>c</sup>  $\pm 200$  Å; measured by electron microscopy in the "dry" state as  $[(\text{BPQ}^{2+})_n \cdot 2n\text{Cl}^-]_{\text{surf}}$ . <sup>d</sup> Calculated from coverage and optical density data: OD/ $\Gamma$ .

Electron microscopy has been used to determine the thickness of the  $[(\text{BPQ}^{2+})_n \cdot 2n\text{Cl}^-]_{\text{surf}}$  on  $\text{SnO}_2$ . Data are included in Table III. Figure 8 shows a representative micrograph showing the glass/ $\text{SnO}_2/[(\text{BPQ}^{2+})_n \cdot 2n\text{Cl}^-]_{\text{surf}}$ . This micrograph is for a glass/ $\text{SnO}_2$  electrode that was

TABLE IV: Electrochemical Potential of Aqueous and Electrostatically Bound Complex Anions

complex	$E^{\circ}$ , <sup>a</sup> V vs. SCE	
	soln	bound to [(BPQ <sup>2+</sup> ) <sub>n</sub> ] <sub>surf</sub>
Fe(CN) <sub>6</sub> <sup>3-/4-</sup>	+0.19 ± 0.02	+0.18 ± 0.03
Ru(CN) <sub>6</sub> <sup>3-/4-</sup>	+0.70 ± 0.02	+0.71 ± 0.03
Mo(CN) <sub>6</sub> <sup>3-/4-</sup>	+0.57 ± 0.02	+0.57 ± 0.03
IrCl <sub>6</sub> <sup>2-/3-</sup>	+0.65 ± 0.02	+0.67 ± 0.03

<sup>a</sup>  $E^{\circ}$  for the indicated couple dissolved in H<sub>2</sub>O at 25 °C or confined within [(BPQ<sup>2+</sup>)<sub>n</sub>]<sub>surf</sub> measured for Pt electrodes in 0.1 M KCl by cyclic voltammetry. The  $E^{\circ}$  was taken to be the average of the anodic and cathodic peaks at a scan rate of 100 mV/s.

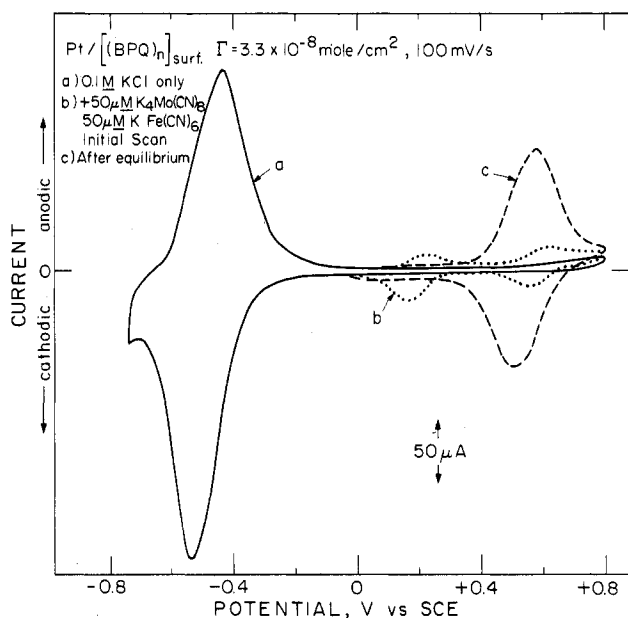


Figure 9. Cyclic voltammetry of Pt electrode derivatized with I showing uptake of Fe(CN)<sub>6</sub><sup>3-/4-</sup> (wave at ~+0.3 V) and Mo(CN)<sub>6</sub><sup>3-/4-</sup> (wave at ~+0.6 V) and ultimate (after ~10 min) equilibrium binding of Mo(CN)<sub>6</sub><sup>3-/4-</sup>.

derivatized with I, cracked, and then examined edge-on. The X-ray analyses of the three regions (glass, SnO<sub>2</sub>, and [(BPQ<sup>2+</sup>)<sub>n</sub>·2nCl<sup>-</sup>]<sub>surf</sub>) clearly show that the micrograph depicts the three material regions. Additionally, the Auger signal intensities (for the same electrode as in Figure 8) while sputtering with Ar<sup>+</sup> ions are consistent with the interface claimed. The film thicknesses for electrodes of known coverage allow a direct measurement of "concentration" of BPQ<sup>2+</sup> units in mol/L. The average value determined for the dry state is ~2.2 M. This value would decrease in solution, assuming that the polymer would be swollen by solvation. The concentration of viologen centers for surface polymers derived from II, measured again in the dry state, is 3.0 M, 50% larger than for the polymer studied here. The lower density of viologen centers in the polymer from I compared to the polymer from II accords well with the conclusion that the benzylviologen centers in [(BPQ<sup>2+/+</sup>)<sub>n</sub>]<sub>surf</sub> are held apart and do not aggregate to give a purple color.

The values of  $D$  in Table II have been calculated by using a concentration of 2.2 M. The values of  $D$  may actually be somewhat higher, since  $D$  is proportional to (concentration)<sup>-1/2</sup> and the polymer would be swollen by solvent. To substantiate the information for the potential step chronoamperometry we have investigated the optical density changes for Pt electrodes derivatized with I. Actually, intensity of reflected 632.8-nm light was measured

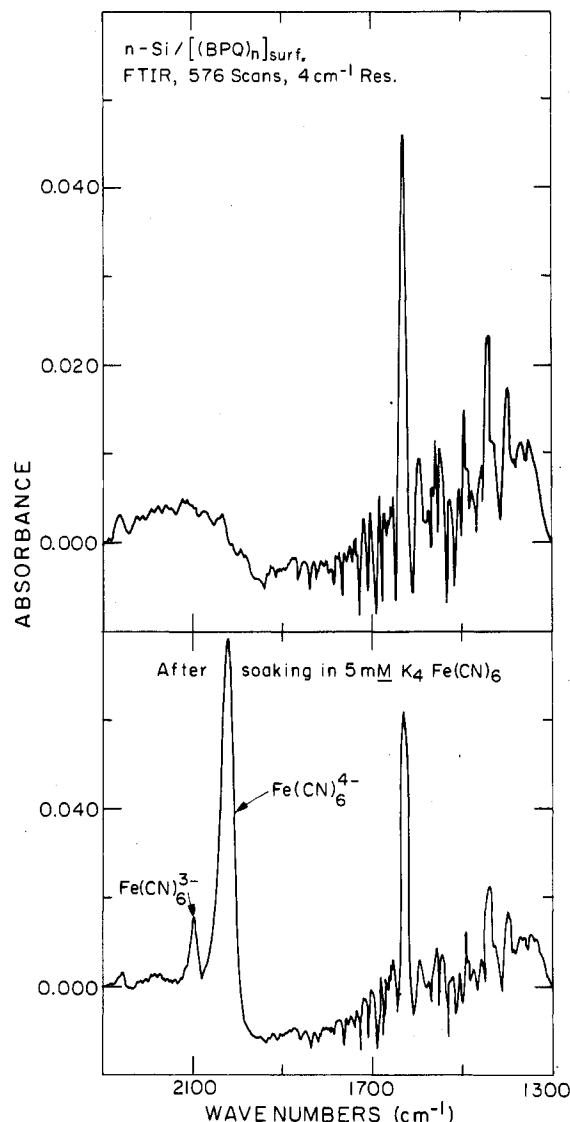


Figure 10. Fourier transform infrared absorption spectrum of n-Si/[(BPQ<sup>2+</sup>)<sub>n</sub>·2nCl<sup>-</sup>]<sub>surf</sub> (top) and after ion exchange with Fe(CN)<sub>6</sub><sup>4-</sup>. The Fe(CN)<sub>6</sub><sup>3-</sup> signal is due to an impurity in the Fe(CN)<sub>6</sub><sup>4-</sup> solution.

as a function of time after a potential step from 0.00 to -0.65 V vs. SCE of Pt/[(BPQ<sup>2+</sup>)<sub>n</sub>]<sub>surf</sub>. The data show that the material on the surface is reduced by 50% at the same time as estimated from an integration of the Cottrell plots, within experimental error. Thus, following a potential step from 0.00 to -0.65 V 50% of the maximum optical density change can be effected in <50 ms for coverages up to 10<sup>-7</sup> mol/cm<sup>2</sup> in aqueous 4.0 M KCl. The [(BPQ<sup>+</sup>)<sub>n</sub>]<sub>surf</sub> → [(BPQ<sup>2+</sup>)<sub>n</sub>]<sub>surf</sub> (blue to colorless) oxidation can be effected with essentially the same time response.

**Electrostatic Binding of Transition-Metal Complexes.** Like surface polymers derived from II,<sup>9</sup> and other electrode-confined polymers having positively charged units, the [(BPQ<sup>2+</sup>)<sub>n</sub>]<sub>surf</sub> polymer will strongly bind large transition-metal complexes.<sup>18</sup> For example, immersion of Pt

(18) (a) Shimomura, T.; Oyama, N.; Anson, F. C. *J. Electroanal. Chem.* 1980, 112, 265. (b) Oyama, N.; Anson, F. C. *J. Electrochem. Soc.* 1980, 127, 247. (c) Oyama, N.; Sato, K.; Matsuda, H. *J. Electroanal. Chem.* 1980, 115, 149. (d) Henning, T. P.; White, H. S.; Bard, A. J. *J. Am. Chem. Soc.* 1981, 103, 3937. (e) Samuels, G. S.; Meyer, T. J. *Ibid.* 1981, 103, 307. (f) Shigehara, K.; Oyama, N.; Anson, F. C. *Ibid.* 1981, 103, 2552. (g) Oyama, N.; Anson, F. C. *Anal. Chem.* 1980, 52, 1192. (h) Facci, J.; Murray, R. W. *J. Phys. Chem.* 1981, 85, 2870. (i) Shigehara, K.; Oyama, N.; Anson, F. C. *Inorg. Chem.* 1981, 20, 518. (j) Buttry, D. A.; Anson, F. C.; *J. Electroanal. Chem.* 1981, 130, 333. (k) Kuo, K.; Murray, R. W. *Ibid.* 1982, 131, 37.

TABLE V: Electrochemical Experimentation To Establish Ordering of Binding of Complex Anions to  $[(BPQ^{2+})_n]_{surf}$ 

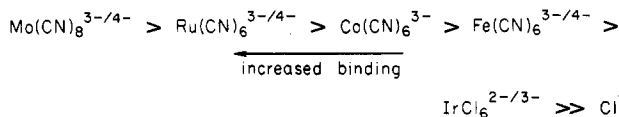
expt	perturbation	response	conclusion
1	dip Pt/ $[(BPQ^{2+})_n \cdot 2nCl^-]_{surf}$ into 0.1 M KCl/50 $\mu$ M $K_2IrCl_6$	$(BPQ^{2+})_n$ wave broadens and shifts negative; $IrCl_6^{2-/3-}$ wave grows in until equal in area to wave for $(BPQ^{2+/+})_n$	$IrCl_6^{2-} \gg Cl^-$
2	add $K_4Fe(CN)_6$ to 50 $\mu$ M in above system	$IrCl_6^{2-/3-}$ wave disappears; wave for $Fe(CN)_6^{3-/4-}$ grows	$Fe(CN)_6^{4-} > IrCl_6^{2-}$
3	add $K_4Mo(CN)_8$ to 50 $\mu$ M in above system	$Fe(CN)_6^{3-/4-}$ wave disappears; wave for $Mo(CN)_8^{3-/4-}$ grows	$Mo(CN)_8^{4-} > Fe(CN)_6^{4-}$
4	add $K_4Ru(CN)_6$ to 50 $\mu$ M in above system	no change in cyclic voltammograms	$Ru(CN)_6^{4-} < Mo(CN)_8^{4-}$
5	dip electrode from expt 4 into saturated KCl for 15 min and scan in 0.1 M KCl containing no other ions	original $(BPQ^{2+/+})_n$ wave regenerated; no other waves detectable	$[(BPQ^{2+})_n \cdot 2nCl^-]_{surf}$ regenerated by ion exchange with excess $Cl^-$
6	dip $[(BPQ^{2+})_n \cdot 2nCl^-]_{surf}$ in 0.1 M KCl/50 $\mu$ M $K_4Mo(CN)_8$ /50 $\mu$ M $K_4Ru(CN)_6$	initially, observe waves for both $Mo(CN)_8^{3-/4-}$ and $Ru(CN)_6^{3-/4-}$ ; but $Mo(CN)_8^{3-/4-}$ signal grows with time while that for $Ru(CN)_6^{3-/4-}$ declines; eventually, only $Mo(CN)_8^{3-/4-}$ signal is observed	$Mo(CN)_8^{3-/4-} > Ru(CN)_6^{4-}$
7	dip $[(BPQ^{2+})_n \cdot 2nCl^-]_{surf}$ into 0.1 M KCl/50 $\mu$ M $K_2IrCl_6$ /50 $\mu$ M $K_4Mo(CN)_8$	initially observe waves for both $IrCl_6^{2-/3-}$ and $Mo(CN)_8^{3-/4-}$ ; but that for $Mo(CN)_8^{3-/4-}$ grows rapidly while that for $IrCl_6^{2-/3-}$ declines; eventually, only wave for $Mo(CN)_8^{3-/4-}$ is observed	$Mo(CN)_8^{4-} > IrCl_6^{2-}$
8	dip $[(BPQ^{2+})_n \cdot 2nCl^-]_{surf}$ into 0.1 M KCl/50 $\mu$ M $K_4Fe(CN)_6$ /50 $\mu$ M $K_4Ru(CN)_6$	observe waves growing for both $Ru(CN)_6^{3-/4-}$ ; but eventually signal for $Fe(CN)_6^{3-/4-}$ continues to grow; at equilibrium signals for both are observed with that for $Ru(CN)_6^{3-/4-}$ dominating	$Ru(CN)_6^{4-} > Fe(CN)_6^{4-}$
9	dip $[(BPQ^{2+})_n]_{surf}$ containing $Fe(CN)_6^{3-}$ into 0.1 M KCl/50 $\mu$ M $K_3Fe(CN)_6$ /50 $\mu$ M $K_3Co(CN)_6$	wave for $Fe(CN)_6^{3-/4-}$ declines to less than 50% of its initial size	$Co(CN)_6^{3-} > Fe(CN)_6^{3-}$

electrodes into an aqueous 0.1 M KCl solution containing 50  $\mu$ M  $IrCl_6^{2-}$  gives negligible response for the  $IrCl_6^{2-/3-}$  redox couple. However, Pt/ $[(BPQ^{2+})_n]_{surf}$  electrodes in the same medium give a cyclic voltammogram consistent with complete charge compensation of the bound  $BPQ^{2+}$  centers by the  $IrCl_6^{2-/3-}$ . That is, a cyclic voltammogram for the polymer-bound  $IrCl_6^{2-} \rightleftharpoons IrCl_6^{3-}$  interconversion has about the same area as for the  $[(BPQ^{2+})_n]_{surf} \rightleftharpoons [(BPQ^+)_n]_{surf}$  interconversion. Immersion of Pt/ $[(BPQ^{2+})_n]_{surf}$  into solutions of other electroactive metal complexes,  $Fe(CN)_6^{3-/4-}$ ,  $Ru(CN)_6^{3-/4-}$ , and  $Mo(CN)_8^{3-/4-}$ , yields similar results. Table IV summarizes the  $E^o$ 's for the solution and surface-bound metal complexes. As reported previously for polymers derived from II,<sup>9</sup> the  $E^o$ 's are the same for the surface-bound species as for the solution species. This fact is consistent with the conclusion that the oxidized and reduced form of a given couple interact equally with the  $(BPQ^{2+})_n$  polymer.

The various complexes, however, do vary in the strength of their binding to  $(BPQ^{2+})_n$ . To establish the relative order of their binding to  $[(BPQ^{2+})_n]_{surf}$ , competition experiments were performed in three stages to ensure that the observed equilibrium situation is internally consistent. For example, to determine whether  $Mo(CN)_8^{4-}$  or  $Fe(CN)_6^{4-}$  binds more strongly to  $[(BPQ^{2+})_n]_{surf}$ , the electrochemical response for a Pt electrode functionalized with I ( $\sim 3 \times 10^{-8}$  mol/cm<sup>2</sup>) after immersion into a 0.1 M KCl/50  $\mu$ M  $Mo(CN)_8^{4-}$ /50  $\mu$ M  $Fe(CN)_6^{4-}$  solution was monitored (Figure 9). Initially, the cyclic voltammetry shows signals for both  $Mo(CN)_8^{4-}$  and  $Fe(CN)_6^{4-}$ , but during the first few cycles the signal for  $Mo(CN)_8^{4-}$  grows while that for  $Fe(CN)_6^{4-}$  declines. The second stage involved starting with a solution containing only 0.1 M KCl and 50  $\mu$ M  $Fe(CN)_6^{4-}$ . After the  $Fe(CN)_6^{4-}$  signal indicated complete incorporation,  $K_4Mo(CN)_8$  was added, making the solution 50  $\mu$ M in  $Mo(CN)_8^{4-}$  at which time the  $Fe(CN)_6^{4-}$  signal was observed to decline and the  $Mo(CN)_8^{4-}$  signal to grow. And finally, the last step involves starting

with a 0.1 M KCl/50  $\mu$ M  $Mo(CN)_8^{4-}$  solution to which  $Fe(CN)_6^{4-}$  is later added. The electrochemical response for  $Mo(CN)_8^{4-}$  always dominates. For all three steps, after 10 min, equilibrium is established with  $Mo(CN)_8^{4-}$  incorporated to the extent that it totally charge compensates the polymer. These experiments suggest that, while  $Fe(CN)_6^{4-}$  may be as fast getting into the polymer,  $Mo(CN)_8^{4-}$  is more firmly bound.

By observing the decrease in signal for a bound, electrochemically active anion upon addition of an electrochemically inactive partner (i.e.,  $Co(CN)_6^{3-}$ ) we can include such in our investigation. A compilation of the results from cyclic voltammetry of Pt/ $[(BPQ^{2+})_n]_{surf}$  electrodes is shown in Table V which has allowed us to establish the ordering of the electrostatic binding for several complex anions by  $[(BPQ^{2+})_n]_{surf}$ . The relative ordering is as follows:



It is interesting to note that this is the same ordering found for the polymer derived from II.<sup>9</sup>

In a previous study of the binding of anions to the polymer derived from II, Auger spectroscopy was shown to be a viable tool to determine the relative importance of competing charge-compensating ions.<sup>9</sup> No detailed study of the Auger of the  $[(BPQ^{2+})_n]_{surf}$  system has been performed, but the Auger/depth profile analysis of the electrode shown in Figure 8 reveals a Cl/C ratio about that expected for complete charge compensation of the  $BPQ^{2+}$  units by  $Cl^-$ . It would appear that Auger can be used to analyze the surface-bound polymers from I without severe damage from the analyzing beam. The binding of the metal cyanides to charge compensate the  $BPQ^{2+}$  units can be detected by Fourier transform infrared absorption spectroscopy (Figure 10). Transmission spectra can be obtained for n-Si/ $[(BPQ^{2+})_n]_{surf}$  charge compensated with

TABLE VI: Infrared Bands for C≡N Stretch in Metal Cyanide Complexes Bound by [(BPQ<sup>2+</sup>)<sub>n</sub>]<sub>surf</sub>

complex	band max, cm <sup>-1</sup>	complex	band max, cm <sup>-1</sup>
Fe(CN) <sub>6</sub> <sup>3-</sup>	2104	Ru(CN) <sub>6</sub> <sup>4-</sup>	2036
Co(CN) <sub>6</sub> <sup>3-</sup>	2114	Mo(CN) <sub>6</sub> <sup>4-</sup>	2097
Fe(CN) <sub>6</sub> <sup>4-</sup>	2027		

Cl<sup>-</sup> or with Fe(CN)<sub>6</sub><sup>3-/4-</sup>. Other metal cyanides can be detected as well (Table VI) and the infrared measurements can be used to independently order the binding of the various complexes. The procedure involves determining the relative absorbance for a given complex after equilibration of the n-Si/[(BPQ<sup>2+</sup>)<sub>n</sub>]<sub>surf</sub> with a particular anion-containing solution. The same ordering as determined electrochemically is found by using the infrared technique. The value of the infrared technique is that the species to be detected need not be electroactive, e.g., Co(CN)<sub>6</sub><sup>3-</sup>.

### Summary

Species I is an easily prepared surface-derivatizing reagent that can yield a surface-bound polymer, [(BPQ<sup>2+</sup>)<sub>n</sub>]<sub>surf</sub>, that is durable and redox active. The one-electron reduced state is particularly durable but the two-electron reduced state does not persist in aqueous electrolytes. The [(BPQ<sup>+</sup>)<sub>n</sub>]<sub>surf</sub> is blue (λ<sub>max</sub> = 610 nm), not purple as for the polymer from II (λ<sub>max</sub> = 545 nm), consistent with smaller interactions of the BPQ<sup>+</sup> units than for the units of the polymer from II. The smaller interactions of the BPQ<sup>+</sup> units and the need for a break-in period for polymers derived from I (and not from II) are

both consistent with the conclusion that the polymer from I is more rigid than the polymer from II. However, the order of binding of a series of transition-metal complexes is the same for the polymers from I and II. Further, the polymers, Γ > 3 × 10<sup>-8</sup> mol/cm<sup>2</sup>, derived from reagents I and II are reduced with approximately the same rate upon a potential step to a potential negative of E<sup>o'</sup> for [(BPQ<sup>2+/+</sup>)<sub>n</sub>]<sub>surf</sub>. Apparently, the additional rigidity imposed by the benzyl group of I compared to the propyl group of II is offset by the fact that the benzyl group is unsaturated and may promote charge transport. It is especially noteworthy that the [(BPQ<sup>2+</sup>)<sub>n</sub>]<sub>surf</sub> can be >50% reduced to [(BPQ<sup>+</sup>)<sub>n</sub>]<sub>surf</sub> in <50 ms for Γ ≤ 1 × 10<sup>-7</sup> mol/cm<sup>2</sup>, corresponding to an optical density change of >1.0.

*Acknowledgment.* We thank the U.S. Department of Energy, Office of Basic Energy Sciences, Division of Chemical Sciences, for support of this research. Support from the M.I.T. Laboratory for Computer Science, IBM Fund, is also gratefully acknowledged. Use of the Central Facilities of the Center for Materials Science and Engineering is appreciated.

**Registry No.** I, 87698-68-8; Mo(CN)<sub>6</sub><sup>3-</sup>, 17845-99-7; Mo(CN)<sub>6</sub><sup>4-</sup>, 17923-49-8; Ru(CN)<sub>6</sub><sup>3-</sup>, 54692-27-2; Ru(CN)<sub>6</sub><sup>4-</sup>, 21029-33-4; Co(CN)<sub>6</sub><sup>3-</sup>, 14897-04-2; Fe(CN)<sub>6</sub><sup>3-</sup>, 13408-62-3; Fe(CN)<sub>6</sub><sup>4-</sup>, 13408-63-4; IrCl<sub>6</sub><sup>2-</sup>, 16918-91-5; IrCl<sub>6</sub><sup>3-</sup>, 14648-50-1; Mo(CN)<sub>6</sub><sup>3-</sup>, 38141-22-9; Mo(CN)<sub>6</sub><sup>4-</sup>, 87698-69-9; Pt, 7440-06-4; W, 7440-33-7; Si, 7440-21-3; SnO<sub>2</sub>, 18282-10-5; Cl<sup>-</sup>, 16887-00-6; KCl, 7447-40-7; LiCl, 7447-41-8; K<sub>2</sub>HPO<sub>4</sub>, 7758-11-4; 4,4'-bipyridine, 553-26-4; *p*-(trimethoxysilyl)benzyl chloride, 24413-04-5.

## Ice Melting Induced Phase Transition in Diacyl Phosphatidylcholines<sup>†</sup>

Hector L. Casal,\* David G. Cameron, and Henry H. Mantsch

Division of Chemistry, National Research Council of Canada, Ottawa, Ontario, Canada K1A 0R6 (Received: March 30, 1983)

Infrared studies were made of the gel phases of 1,2-dipalmitoyl- and 1,2-dibehenoyl-*sn*-glycero-3-phosphatidylcholine hydrated with H<sub>2</sub>O and D<sub>2</sub>O. It is shown that ice melting induces a solid-solid phase change in the lipid.

### Introduction

Of late, there has been considerable interest in transitions in the gel phases of fully saturated synthetic lipids. In the phosphatidylcholines<sup>1</sup> and sulfocholines<sup>2</sup> it has been found that incubation near 0 °C results in dehydration of the head group, and a change in the acyl chain packing<sup>2-6</sup>, effects which are almost completely reversed when the temperature is elevated.<sup>6</sup> Two phase transitions have been reported for dilaurylphosphatidylethanolamine;<sup>7</sup> it has since been shown<sup>8</sup> that the dimyristoyl- and dipalmitoylphosphatidylethanolamines also exhibit this behavior and that the transitions result from molecules in different states of hydration.<sup>8-10</sup>

Many such studies encompass the solid-liquid transitions of H<sub>2</sub>O (0 °C) and D<sub>2</sub>O (3.8 °C). Generally, no anomalous behavior of lipid properties has been reported, with two exceptions.<sup>11,12</sup> In this paper we briefly report that the melting of the water in a hydrated diacyl phos-

phatidylcholine gel induces changes in its infrared spectra which are interpreted as a solid-solid phase transition in the lipid.

(1) Chen, S. C.; Sturtevant, J. M.; Gaffney, B. J. *Proc. Natl. Acad. Sci. U.S.A.* 1980, 77, 5060-3.

(2) Mantsch, H. H.; Cameron, D. G.; Tremblay, P. A.; Kates, M. *Biochim. Biophys. Acta* 1982, 689, 63-72.

(3) Fuldner, H. H. *Biochemistry* 1981, 20, 5707-10.

(4) Ruocco, M. J.; Shipley, G. G. *Biochim. Biophys. Acta* 1982, 684, 59-66.

(5) Ruocco, M. J.; Shipley, G. G. *Biochim. Biophys. Acta* 1982, 691, 309-20.

(6) Cameron, D. G.; Mantsch, H. H. *Biophys. J.* 1982, 38, 175-84.

(7) Wilkinson, D. A.; Nagle, J. F. *Biochemistry* 1981, 20, 187-92.

(8) Mantsch, H. H.; Hsi, S. C.; Butler, K. W.; Cameron, D. G. *Biochim. Biophys. Acta* 1983, 728, 325-30.

(9) Chang, H.; Eppard, R. M. *Biochim. Biophys. Acta* 1983, 728, 319-24.

(10) Seddon, J. M.; Harlos, K.; Marsh, D. *J. Biol. Chem.* 1983, 258, 3850-4.

(11) Davis, J. H. *Biophys. J.* 1979, 27, 339-58.

(12) Tardieu, A. Ph.D. Thesis, Université de Paris-Sud, 1972. Cited in Janiak, M. J.; Small, D. M.; Shipley, G. G. *J. Biol. Chem.* 1979, 254, 6068-78.

<sup>†</sup> Issued as NRCC No. 21055.